

# The isotopic and chemical compositions of the CO<sub>2</sub>-rich waters in Korea

Yongkwon Koh, Chunsoo Kim, Daeseok Bae and Kyeongwon Han

Korea Atomic Energy Research Institute, Yuseong, Daejeon, Korea

Received: September 2, 2001; accepted: May 13, 2002.

## RESUMEN

Se investigó la composición química e isotópica de agua rica en CO<sub>2</sub> que se encuentra principalmente en terrenos graníticos de Korea. Las aguas ricas en CO<sub>2</sub> pueden dividirse en tres tipos dependiendo de su composición química: Na-HCO<sub>3</sub>, Ca-Na-HCO<sub>3</sub> y Ca-HCO<sub>3</sub>. La química del agua indica que estas aguas evolucionaron a través de una reacción fuerte con las rocas huésped por una entrada de CO<sub>2</sub> profundo durante la circulación profunda. El proceso de disolución del plagioclasa es importante en las interacciones agua/granito y sus cambios de solubilidad con la temperatura de reacción juegan un rol importante en la determinación de la composición química. Los cálculos de equilibrio multicomponente mineral/agua indican que el agua rica en CO<sub>2</sub> alcanza temperaturas de 115-140 °C.

Los datos de δ<sup>18</sup>O y δD indican que las aguas ricas en CO<sub>2</sub> provienen de agua meteorítica y tienen una composición isotópica más ligera que otras aguas naturales. El contenido de tritio muestra un tiempo de residencia largo y la posibilidad de un flujo de CO<sub>2</sub> en un acuífero a mayor profundidad. También existe una fuerte indicación de mezcla durante su ascenso hacia la superficie entre el agua profunda rica en CO<sub>2</sub> y agua fresca más reciente. Los análisis de isótopos de carbono muestran que la composición del carbono está asociada con CO<sub>2</sub> proveniente del manto. Los datos preliminares de las relaciones de isótopos de helio también indican que el CO<sub>2</sub> se originó en el manto. Las relaciones de isótopos de estroncio indican que la química del agua rica en CO<sub>2</sub> está determinada por la reacción con el granito local.

**PALABRAS CLAVE:** Aguas ricas en CO<sub>2</sub>, química, isotopía, interacción agua-roca, mezcla, geotermometría.

## ABSTRACT

The chemical and isotopic compositions of CO<sub>2</sub>-rich water (P<sub>CO<sub>2</sub></sub> ≈ 1 atm) in Korea mainly occurring in granitic terrain were investigated. CO<sub>2</sub>-rich waters can be divided into three types based on chemical compositions: Na-HCO<sub>3</sub>, Ca-Na-HCO<sub>3</sub> and Ca-HCO<sub>3</sub> types. Water chemistry indicates that these waters were evolved through a strong reaction of the host rocks with a supply of deep-seated CO<sub>2</sub> during deep circulation. The dissolution process of plagioclase is important in water/granite interactions and its solubility changes with reaction temperature played an important role in the determination of chemical composition. Multi-component mineral/water equilibrium calculations indicate that the CO<sub>2</sub>-rich water reaches temperature of 115-140°C.

δ<sup>18</sup>O and δD data indicate that CO<sub>2</sub>-rich waters were derived from local meteoric water and have a lighter isotope composition than other natural waters. The tritium contents show a long residence time and the possibility of CO<sub>2</sub> flux in an aquifer at great depth. There is a strong indication of mixing between deep CO<sub>2</sub>-rich water and recent fresh water during ascent to the surface. Carbon isotope analysis reveals that the carbon composition is associated with mantle-derived CO<sub>2</sub>. The preliminary helium isotope ratio also supports that the CO<sub>2</sub> gas was derived from mantle origin. The strontium isotope ratios indicate that the chemistry of the CO<sub>2</sub>-rich water is determined by reaction with local granite.

**KEY WORDS:** CO<sub>2</sub>-rich water, chemistry, isotope, water/rock interaction, mixing, geothermometry.

## INTRODUCTION

Many thermal and mineralized springs in Korea are generally produced in plutonic rocks and characterized by a low temperature system, resulting from an inactive tectonic setting of the Korean peninsula. A large amount of geological, geophysical, chemical and isotopic data for the thermal water has been collected (Yun *et al.*, 1998; Kim *et al.*, 2000). However, a geochemical study of the mineralized water with high P<sub>CO<sub>2</sub></sub> has recently initiated. The CO<sub>2</sub>-rich waters have

been studied, in terms of hydrogeological setting and general characteristics of water compositions on a regional scale. The detailed studies of the evolution of CO<sub>2</sub>-rich water including origin, water/rock interaction and mixing between CO<sub>2</sub>-rich water and groundwater have been limited.

For the systematic study of the CO<sub>2</sub>-rich water in Korea, the geochemical and isotopic studies on selected sites were carried out as a first step. There are more than 50 CO<sub>2</sub>-rich springs in Korea according to historical record (Figure

1); however, many locations are too remote and widely distributed to access for the investigation. For this study, samples were collected from most of the springs located in inhabited areas. The waters were chemically analyzed and isotopic compositions were determined, including  $^2\text{H}$ ,  $^3\text{H}$ ,  $^{18}\text{O}$ ,  $^{13}\text{C}$ ,  $^{34}\text{S}$ , and  $^{87}\text{Sr}/^{86}\text{Sr}$ . The  $^3\text{He}/^4\text{He}$  ratio of a few samples is also determined. These data are used to elucidate the hydrogeological characteristics of the  $\text{CO}_2$ -rich waters with support of the deep reservoir temperature, estimated from chemical geothermometers and multicomponent equilibrium calculations.

### GEOLOGICAL SETTING

The geology of Korea is characterized by a very complex system with various rock types from Precambrian to

Quaternary. Basement rocks occupying more than half of the Korean peninsula consist of Precambrian metamorphic rocks and Paleozoic-Mesozoic plutonic rocks, which were subjected to several uplift and erosion stages after Cretaceous time (Figure 1). After the Mesozoic tectonic movements, the whole of the peninsula was uplifted. The Cenozoic tectonic activity was not intense and is generally represented by mafic to intermediate volcanic activity in limited areas (Lee, 1999). The arrangement of mountain ranges was primarily influenced by Mesozoic tectonic movements. During this period, intensive folding, faulting, plutonic intrusion, and volcanism became active in East Asia including the Korean peninsula. In the early Mesozoic era, large folds and nappes with an E-W trend were formed and then the tectonic movements in the Jurassic period resulted in the mountains and valleys with NE-SW trends. In the Cretaceous period,

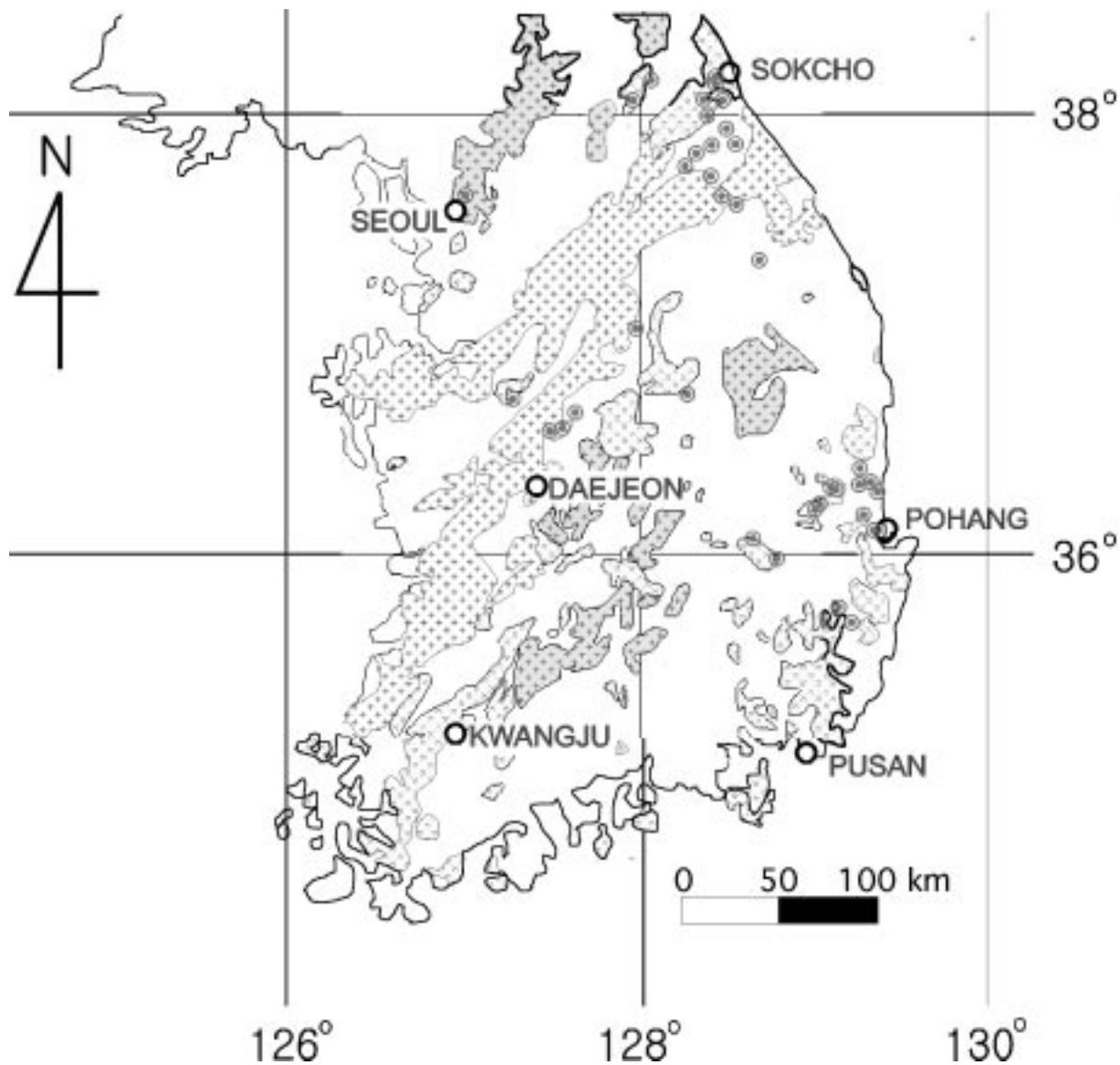


Fig. 1. Geologic map of Korea. Sample locations are also shown.

the Korean direction on a NNW-SSE trend was formed (Lee, 1999). Topographically, the Korean peninsula is a rugged country, having about 70% mountainous terrain. Higher mountains of 1400 to 1600 m above sea level are concentrated in the eastern regions.

Most of the CO<sub>2</sub>-rich springs are concentrated in the eastern region of Korea and located along a marginal area of granites or a fracture system of NNW-SSE trend (Figure 1). Most of the CO<sub>2</sub>-rich waters studied are related to plutonic rocks in the Kangwon province and some sites of the Kyeongsang province, where the water emerges from sedimentary rocks (Figure 1). Even though the CO<sub>2</sub>-rich water from sedimentary origin has not been clearly demonstrated, it is expected that a CO<sub>2</sub>-rich water reservoir is likely to be located in the basement underlying the sedimentary terrain.

### SAMPLING AND ANALYTICAL PROCEDURE

Sampling of various kinds of natural waters (CO<sub>2</sub>-rich groundwater, groundwater and surface water) from 47 locations (Figure 1) was carried out between May 1997 and November 2000 (Table 1). Most of the CO<sub>2</sub>-rich waters are from natural springs and a few from deep drillholes in depths ranging from 400 to 650 m. Field measurements including temperature, pH, Eh, dissolved oxygen, electrical conductivity and alkalinity were carried out.

Major dissolved ionic constituents in waters were analyzed at the Korea Basic Science Institute (KBSI) using an inductively coupled plasma mass spectrometry (ICP-MS; Fisons-PlasmaTrace) for cations and at the Korea Atomic Energy Research Institute (KAERI) with the ion chromatography (Dionex 500) for anions. The  $\delta^{18}\text{O}$  and  $\delta\text{D}$  values of waters were determined using a stable isotope ratio mass spectrometry (VG SIRA II and Micromass OPTIMA) at KAERI. The bicarbonates were precipitated in the field using NaOH and BaCl<sub>2</sub> solution for the analysis of  $\delta^{13}\text{C}$ . The  $\delta^{34}\text{S}$  values of dissolved SO<sub>4</sub> in waters were measured at the Institute of Mineral Deposits of China at Beijing by Finnigan MAT 230C. The tritium contents of waters were measured at the KAERI by a liquid scintillation counter (Packard 2770TR/SL) after the electrolytic enrichment process. Strontium isotopic ratios were measured at the KBSI by TIMS (VG Sector 54-30). The <sup>3</sup>He/<sup>4</sup>He ratios are preliminarily measured by VG5400 at Seoul National University. The samples were collected using copper tubes, sealed by cold welding. The thermodynamic calculations including the mineral saturation indices were calculated using the SOLVEQ computer program (Reed, 1982).

### WATER CHEMISTRY

In situ measurement data and chemical compositions of the representative water samples from the study area are summarized in Table 1. The most distinctive property of the

CO<sub>2</sub>-rich water is a high CO<sub>2</sub> partial pressure value ( $P_{\text{CO}_2} < 10^{0.31}\text{atm}$ ). The temperature of discharging CO<sub>2</sub>-rich springs is low (20°C is maximum value), whereas the well-head temperature of borehole CO<sub>2</sub>-rich water is in the ranges of 25-35°C. The pH of all CO<sub>2</sub>-rich waters ranges from 5.5 to 6.4. The flow rates of CO<sub>2</sub>-rich springs are usually small, frequently below 0.1L/s. The CO<sub>2</sub>-rich waters have very high content of dissolved solids (up to 3300 mg/L).

The Ca, Na and HCO<sub>3</sub> concentrations in the CO<sub>2</sub>-rich water are dominant. Mg, K, Cl, SO<sub>4</sub>, Fe and Sr concentrations in the water are also enriched, though Cl and SO<sub>4</sub> concentrations are low (Table 1). High CO<sub>2</sub> gas concentrations of the CO<sub>2</sub>-rich waters are ascribed to accelerate the water rock interaction. Enhanced water/rock reaction under a low pH condition leads to the dissolution of selected minerals in surrounding rocks and consequently, Ca, Na, Mg, K and HCO<sub>3</sub> concentrations are enriched in the CO<sub>2</sub>-rich groundwater. Their water composition can be divided into three main groups based on chemical compositions: Na-HCO<sub>3</sub>, Ca-Na-HCO<sub>3</sub> and Ca-HCO<sub>3</sub> types (Figure 2). Na, K and SiO<sub>2</sub> are dominant in a Na-HCO<sub>3</sub> type, whereas Ca, Mg and Fe are dominant in a Ca-HCO<sub>3</sub> type (Table 1).

Ca and Na in natural waters are commonly derived by the dissolution of plagioclase in a granitic terrain. The plagioclase composition of all granites ranges from Ab<sub>80</sub> to Ab<sub>60</sub>. However, the CO<sub>2</sub>-rich water of Ca-HCO<sub>3</sub> type is more enriched in Ca (up to 170.0 mg/l) than Na (up to 34.5mg/l), suggesting that the water chemistry could not be simply explained by the stoichiometric dissolution of plagioclase.

Dissolution of calcite may also contribute to Ca content in the waters. The hydrothermal calcite or secondary calcite from a weathering process can be distributed throughout the granitic rocks. If the CO<sub>2</sub>-rich water was continuously reacting with calcites during uprising to the surface with an undersaturation with respect to calcite, the saturation index of the CO<sub>2</sub>-rich water will be close to zero value. However, it is unlikely that the dissolution of calcite was mainly contributed to CO<sub>2</sub>-rich water of Ca-HCO<sub>3</sub> type, although most of the CO<sub>2</sub>-rich water are saturated or supersaturated with respect to calcite. CO<sub>2</sub>-rich water was supersaturated with respect to calcite in depth and the saturation state is likely controlled by the extent of mixing process with fresh water. The strontium isotope compositions of the waters and accompanying minerals of certain locations show that the carbonate mineral does not contribute to Ca content in the CO<sub>2</sub>-rich water. Therefore, the Ca enrichment is likely to be controlled by other mechanism. The solubility difference between albite and anorthite is likely to be a possible explanation of Ca enrichment in the CO<sub>2</sub>-rich water of Ca-HCO<sub>3</sub> type. The CO<sub>2</sub>-rich water in Korea is chemically characterized as Na-HCO<sub>3</sub> and Ca-HCO<sub>3</sub> types in a similar geological setting. For explanation of Na-HCO<sub>3</sub> type in CO<sub>2</sub>-

**Table 1**  
 Geochemical and isotopic data of the representative CO<sub>2</sub>-rich waters in Korea.

| Sample no. | Temp. (°C) | pH  | TDS (mg/L) | Concentration (mg/L) |      |       |       |                  |            |       | Log PCO <sub>2</sub> (atm) | δ <sup>18</sup> O (‰) | δD (‰) | δ <sup>13</sup> C (‰) | δ <sup>34</sup> S (‰) | Tritium (TU) | <sup>87</sup> Sr/ <sup>86</sup> Sr |
|------------|------------|-----|------------|----------------------|------|-------|-------|------------------|------------|-------|----------------------------|-----------------------|--------|-----------------------|-----------------------|--------------|------------------------------------|
|            |            |     |            | Na                   | K    | Mg    | Ca    | SiO <sub>2</sub> | Alkalinity |       |                            |                       |        |                       |                       |              |                                    |
| KW-1"      | 6.5        | 6.4 | 2358       | 565.1                | 12.0 | 1.5   | 66.1  | 94.4             | 1595       | -0.05 | -10.8                      | -76.9                 | -3.7   | -                     | 5.6                   | -            |                                    |
| KW-2'      | 18.2       | 6.2 | 2625       | 544.0                | 32.1 | 2.6   | 57.1  | 93.1             | 1861       | 0.00  | -11.7                      | -83.3                 | -8.3   | 10.7                  | 1.7                   | 0.724520     |                                    |
| KW-4"      | 7.9        | 6.7 | 3091       | 460.0                | 10.0 | 4.9   | 51.7  | 58.6             | 2470       | -0.43 | -11.3                      | -81.6                 | -7.2   | 24.6                  | 1.1                   | -            |                                    |
| KW-8       | 14.5       | 5.5 | 714        | 71.4                 | 4.5  | 7.3   | 76.1  | 32.5             | 488        | -0.05 | -10.4                      | -72.7                 | -8.8   | 12.0                  | 7.6                   | 0.726720     |                                    |
| KW-9       | 17.6       | 5.9 | 1104       | 113.0                | 3.8  | 21.3  | 152.0 | 38.1             | 670        | -0.14 | -10.8                      | -78.5                 | -11.5  | 11.0                  | 3.4                   | -            |                                    |
| KW-5'      | 6.9        | 6.1 | 1076       | 38.1                 | 2.9  | 25.9  | 314.6 | 61.8             | 1055       | -0.11 | -10.1                      | -72.3                 | -6.1   | 8.0                   | 7.6                   | -            |                                    |
| KW-8       | 5.7        | 6.4 | 1453       | 60.8                 | 4.9  | 31.8  | 361.8 | 98.4             | 1435       | -0.12 | -10.8                      | -84.1                 | -3.6   | 7.4                   | 10.2                  | -            |                                    |
| KW-12      | 16.2       | 5.8 | 856        | 14.8                 | 1.6  | 36.1  | 140.0 | 35.1             | 598        | -0.10 | -10.8                      | -81.7                 | -4.6   | 5.0                   | 9.6                   | -            |                                    |
| S1         | 16.9       | 6.3 | 1,519      | 184.0                | 6.8  | 45.3  | 153.0 | 35.9             | 1033       | -0.35 | -8.4                       | -63.0                 | -4.9   | 7.3                   | 5.8                   | -            |                                    |
| S6         | 12.8       | 6.3 | 3,144      | 318.0                | 9.7  | 79.1  | 391.0 | 82.6             | 2167       | -0.07 | -10.6                      | -73.9                 | -      | -                     | 1.3                   | -            |                                    |
| G2         | 17.2       | 6.2 | 1450       | 60.6                 | 3.0  | 43.0  | 231.0 | 56.5             | 961        | -0.27 | -8.7                       | -55.1                 | -5.4   | 6.5                   | 4.7                   | -            |                                    |
| G4         | 8.6        | 6.2 | 3769       | 114.3                | 13.9 | 89.3  | 673.5 | 116.5            | 2694       | -0.09 | -9.6                       | -66.7                 | -1.9   | -                     | 0.6                   | -            |                                    |
| G5         | 14.4       | 6.3 | 1897       | 80.9                 | 4.3  | 65.2  | 252.0 | 73.6             | 1388       | -0.26 | -10.0                      | -66.8                 | -7.3   | -                     | 1.1                   | -            |                                    |
| G8         | 16.0       | 6.3 | 3096       | 154.0                | 7.5  | 108.0 | 450.0 | 96.9             | 2196       | -0.25 | -9.9                       | -73.7                 | -2.1   | -                     | 0.0                   | -            |                                    |
| J1         | 29.4       | 6.3 | 3306       | 300.0                | 18.0 | 44.0  | 464.0 | 102.7            | 2327       | -0.03 | -10.4                      | -72.3                 | 0.0    | 0.3                   | -                     | -            |                                    |
| J1"        | 28.4       | 6.3 | 2721       | 245.0                | 11.3 | 39.5  | 363.0 | 96.9             | 1895       | 0.38  | -10.5                      | -72.0                 | 0.1    | -3.1                  | 27.6                  | 0.719502     |                                    |
| J2         | 19.5       | 5.7 | 2009       | 118.0                | 2.6  | 36.3  | 276.0 | 81.3             | 1464       | 0.09  | -9.8                       | -69.4                 | 0.5    | -4.7                  | -                     | 0.716914     |                                    |
| H-1a       | 30.2       | 6.4 | 521        | 86.6                 | 3.2  | 41.8  | 364.4 | 24.8             | 1452       | -0.27 | -9.9                       | -70.5                 | -      | 6.1                   | 0.3                   | -            |                                    |
| H-2a       | 29.2       | 5.9 | 562        | 80.5                 | 2.6  | 35.3  | 316.0 | 127.8            | 1281       | 0.17  | -10.1                      | -75.4                 | -2.0   | -                     | 0.1                   | 0.714812     |                                    |
| CJ-1       | 18.9       | 5.4 | 660        | 30.7                 | 2.8  | 20.7  | 115.0 | 41.5             | 458        | 0.26  | -8.3                       | -58.2                 | -5.3   | 5.2                   | 6.0                   | 0.714621     |                                    |
| CJ-4       | 16.7       | 5.1 | 295        | 25.2                 | 3.3  | 7.3   | 46.2  | 37.2             | 185        | 0.09  | -8.3                       | -58.9                 | -5.3   | 7.0                   | 7.6                   | -            |                                    |
| CJ-19      | 15.2       | 5.5 | 966        | 28.0                 | 2.1  | 28.9  | 170.0 | 56.0             | 689        | 0.21  | -8.5                       | -60.9                 | -7.8   | -                     | 4.6                   | 0.723842     |                                    |

rich water, it can be considered that the solubility difference between anorthite and albite decreases dramatically with increasing reaction temperature. Thus the dissolution process of plagioclase is important in water-granite interactions and its solubility change with a reaction temperature plays an important role in the determination of chemical compositions. Therefore, it can be interpreted that the recognized chemical difference was mainly due to the difference of reaction temperature.

Additionally, the CO<sub>2</sub>-rich water in a sedimentary terrain shows the similar characteristics of the CO<sub>2</sub>-rich water in a granitic terrain. It supports that the CO<sub>2</sub>-rich water is saturated with respect to calcite in depth, where host rocks are granites underlying the sedimentary rocks. Therefore, the reaction of CO<sub>2</sub>-rich water with sedimentary rocks was limited, specially with carbonate minerals.

### ISOTOPIC CHARACTERISTICS

The δ<sup>18</sup>O versus δD diagram indicates that all kinds of waters from the study area were derived from local meteoric waters (Figure 3). Figure 3 also shows that the CO<sub>2</sub>-rich wa-

ter has a wide range of isotopic compositions. The δ<sup>18</sup>O and δD values of some CO<sub>2</sub>-rich water can not be distinctly discriminated from those of shallow groundwater and surface water. This indicates that the mixing process occurred in a great extent between CO<sub>2</sub>-rich water and superficial water. The CO<sub>2</sub>-rich water from drillholes is plotted toward more negative δ<sup>18</sup>O values with respect to the local meteoric water line (Figure 3). Although the oxygen shift is small, this shift can be explained as a consequence of isotope re-equilibrium with CO<sub>2</sub> gas.

δ<sup>18</sup>O tends to have a negative correlation with TDS and a positive correlation with tritium (Figure 4). It is noteworthy that the tritium contents close to zero are observed only in the Na-HCO<sub>3</sub>, confirming a long residence time and the possibility of a CO<sub>2</sub> inflow in an aquifer at great depth. This strongly suggests that the Ca-HCO<sub>3</sub> type of CO<sub>2</sub>-rich water was mixed with shallow groundwater and/or surface water during ascending at depth, whereas the Na-HCO<sub>3</sub> type water was less mixed with surface water.

The δ<sup>13</sup>C values of the CO<sub>2</sub>-rich water, groundwater and surface water show a distinct difference (Table 1). The pos-

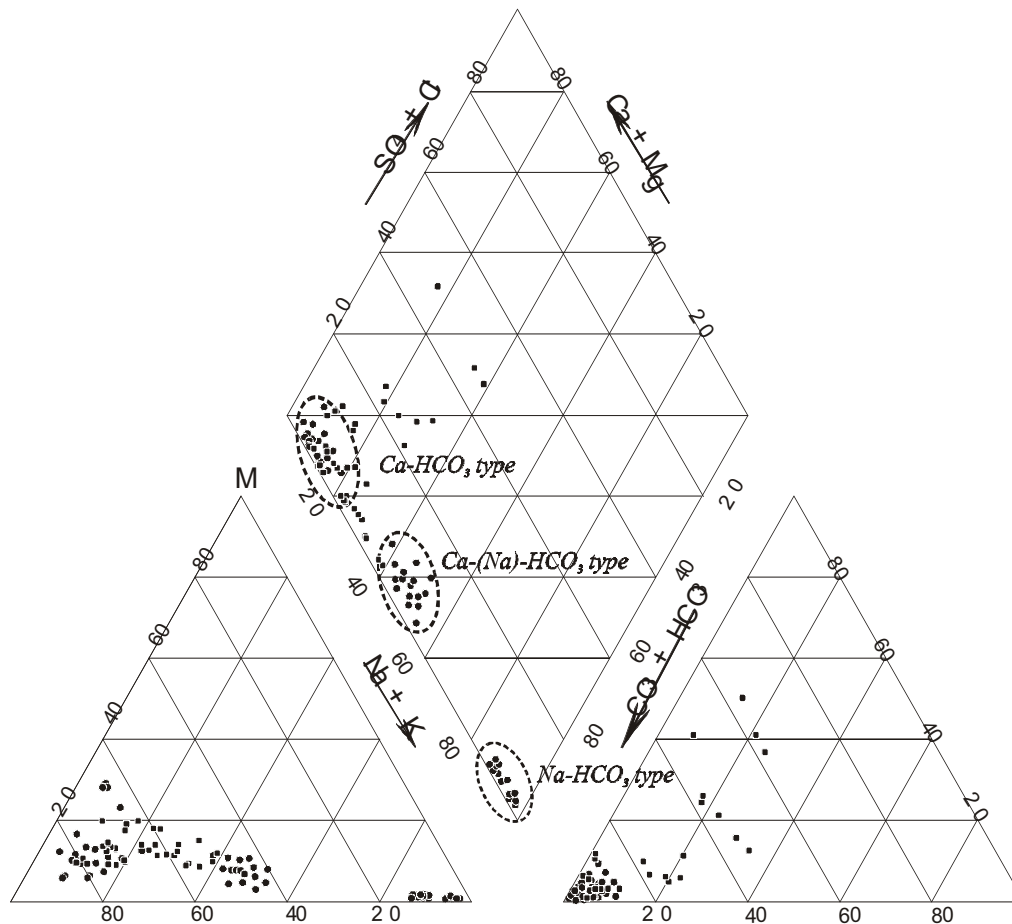


Fig. 2. Piper's diagram showing chemical compositions of the CO<sub>2</sub>-rich waters in Korea.

sible sources of carbon in the CO<sub>2</sub>-rich water with relatively enriched δ<sup>13</sup>C may be the dissolution of carbonate rock and deep-seated CO<sub>2</sub> gas (Deines and Gold, 1973) (Figure 5). Relationship between δ<sup>18</sup>O and δD of the CO<sub>2</sub>-rich water indicates the re-equilibrium with CO<sub>2</sub> gas rather than the reaction with vein calcite. Additionally, the result of the strontium isotope analysis is not consistent with the dissolution of calcite. The preliminary helium isotope analysis (R/Ra=1.2) supports the possibility of mantle-derived CO<sub>2</sub> as source of CO<sub>2</sub> gas.

The δ<sup>34</sup>S values of dissolved sulfate of all kinds of waters range widely from +3.6 to +37.6‰ (Figure 5). It is noteworthy that the δ<sup>34</sup>S values of certain CO<sub>2</sub>-rich water are much higher than those of other type waters. This probably reflects the different source(s) of sulfur in waters and different isotopic fractionation mechanism for sulfur-sulfate in the subsurface. The enriched δ<sup>34</sup>S<sub>SO4</sub> values (up to +38‰) of the CO<sub>2</sub>-rich water strongly indicate that the sulfate reduction by organic activity had occurred at depth.

The Sr concentration of the water varies from 0.02 to 2.8 mg/l and the CO<sub>2</sub>-rich water exhibits a wide range in <sup>87</sup>Sr/<sup>86</sup>Sr value (0.7146-0.7267). Although we could not obtain the strontium isotopic composition of rock-forming minerals from granite, the values indicate that the strontium isotope ratio of the CO<sub>2</sub>-rich water is similar to the value of local granite. Because the most common calcium-bearing mineral in granite is plagioclase, the result suggests that the calcium source is mainly plagioclase, and the CO<sub>2</sub>-rich water might be evolved from the reaction with granite at depth. It could be clearly explained by the further study for strontium isotopic composition of each mineral of granite.

### GEOTHERMOMETRY

Various chemical geothermometers have been developed to predict the reservoir temperatures in geothermal system (Arnorrsson, 1983; Giggenbach, 1988). Because they use only a few chemical components analyzed, variable temperatures can be frequently predicted for a same fluid. These temperature variations may be due to the lack of equilibrium between solutes and minerals or due to additional processes (including mixing with cold water in the upflow). Reed and Spycher (1984) showed that a reliable estimate of reservoir temperature could be obtained by considering simultaneously the state of equilibrium between specific water and many geothermal minerals as a function of temperature. We applied the multicomponent mineral equilibrium approach to sample J1 of CO<sub>2</sub>-rich water, yielding the log Q/K vs. temperature diagram (Figure 6). The mineral equilibrium geothermometer temperatures, therefore the probable reservoir temperatures, are estimated to be about

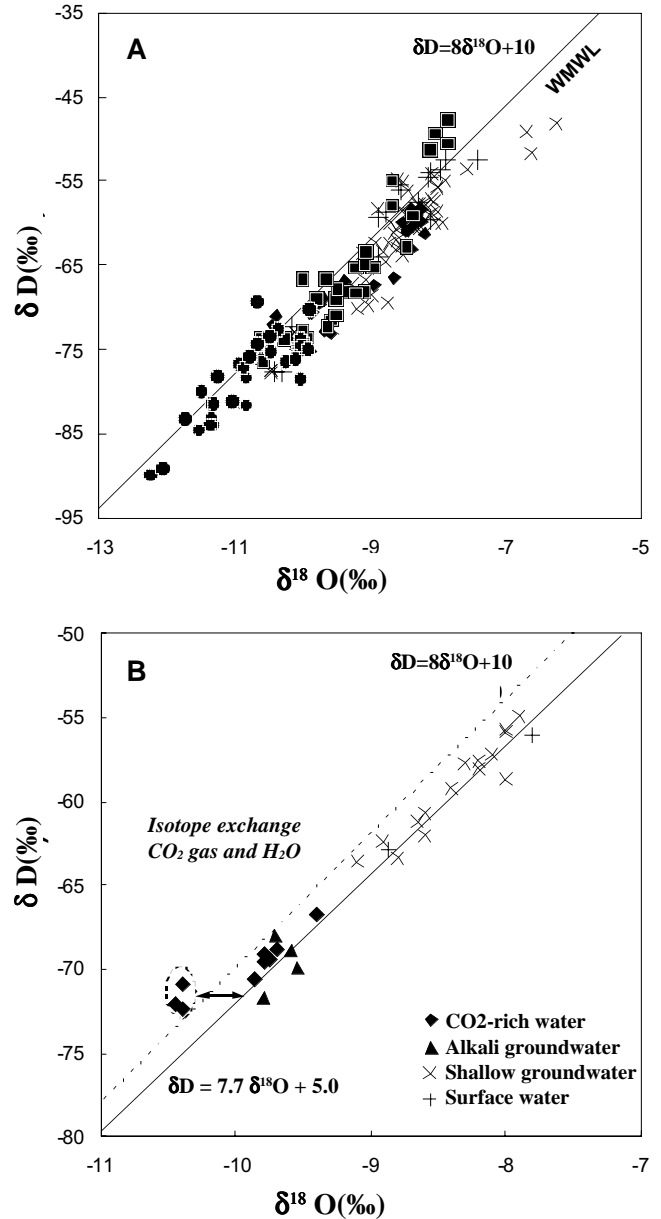


Fig. 3. δ<sup>18</sup>O vs δD diagram of the CO<sub>2</sub>-rich waters including groundwater and surface water.

115° to 140°C (Figure 6). In comparison, the other calculated temperatures for the sample J1 are 143° to 195°C from Na-K geothermometers (Arnorrsson, 1983; Giggenbach, 1988).

### DISCUSSION AND CONCLUSION

The CO<sub>2</sub>-rich water in Korea is represented by the mineralized water with low pH (5.5-6.5), high concentrations of Ca, Na, HCO<sub>3</sub> (up to 3300 mg/L, TDS) and low concentration of Cl and SO<sub>4</sub>. Although the discharging temperature of the CO<sub>2</sub>-rich water is low, the water chemistry indicates that

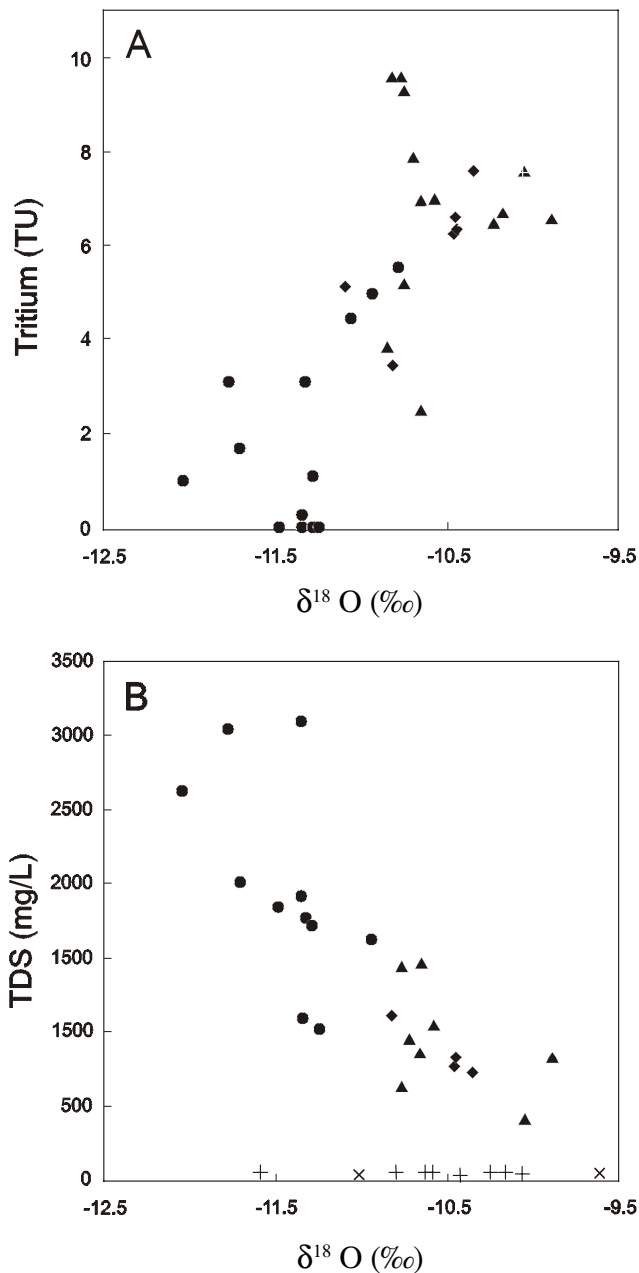


Fig. 4. Plots of  $\delta^{18}\text{O}$  versus A) tritium and B) TDS for the CO<sub>2</sub>-rich waters of Kangwon province in Korea.

the geothermal system exist beneath the study areas. The CO<sub>2</sub>-rich waters can be divided into three chemical types (Na-HCO<sub>3</sub>, Ca-Na-HCO<sub>3</sub> and Ca-HCO<sub>3</sub> types). Although the solubility difference between albite and anorthite with reaction temperature is applied for explaining these chemical differences, the sophisticated thermodynamical approach is required for successful interpretation. Strontium isotope measurements support that the CO<sub>2</sub>-rich water was evolved with local-host (granite) rock reaction. The relationship between  $\delta^{18}\text{O}$  and  $\delta\text{D}$  values and tritium content of water indicate that

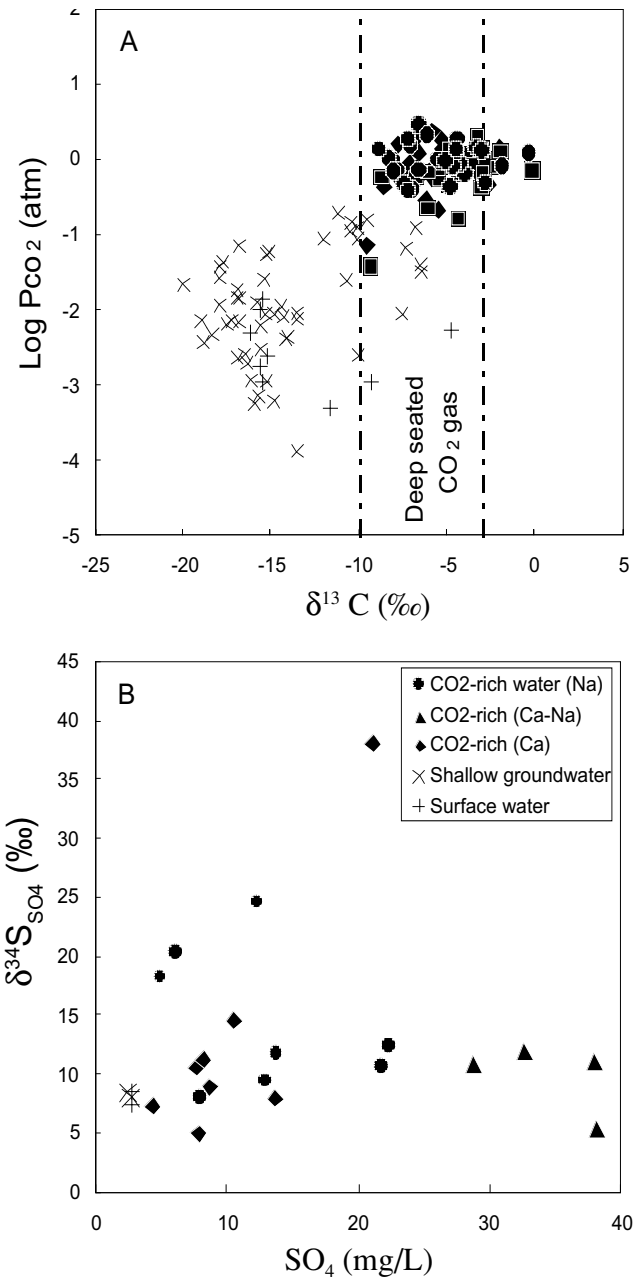


Fig. 5. A) Plots of  $\delta^{13}\text{C}$  versus Log Pco<sub>2</sub> (atm) for the water samples. B) Plots of SO<sub>4</sub> (mg/L) versus  $\delta^{34}\text{S}$  for the CO<sub>2</sub>-rich waters in Korea.

the mixing process occurred between CO<sub>2</sub>-rich water and shallow groundwater during fluid ascending. Some samples from borehole show isotopic re-equilibrium with CO<sub>2</sub> gas at depth. Carbon isotope composition of the CO<sub>2</sub>-rich water shows a range associated mantle derived CO<sub>2</sub>. Although <sup>3</sup>He/<sup>4</sup>He ratios of a few water samples are low ( $R/R_a = 1.2$ ), they suggest the presence of a mantle source. However, further study is necessary to clarify the CO<sub>2</sub> source. Higher  $\delta^{34}\text{S}$  value of dissolved sulfate showing sulfate reduction argues against higher Fe concentration and no existence of hydrogen sulfide.

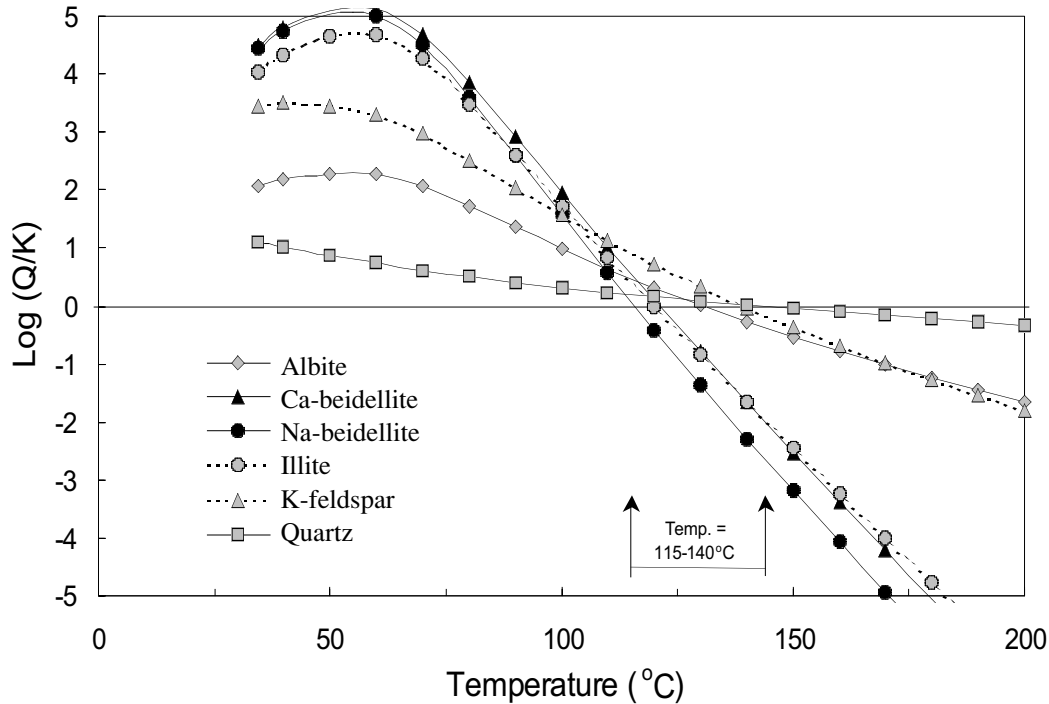


Fig. 6. A temperature versus log Q/K diagram showing the coprecipitation equilibrium condition for alteration minerals (for the sample J1). The probable equilibrium temperature is about 115 to 140°C, which is much higher than the well head temperature (35°C).

**BIBLIOGRAPHY**

ARNORSSON, S., 1983. Chemical equilibria in Icelandic geothermal systems - Implications for chemical geothermometry investigations. *Geothermics*, 12, 119-128.

DEINES, P. and D. P. GOLD, 1973. The isotopic composition of carbonatite and kimberlite carbonates and their bearing on the isotopic composition of deep-seated carbon. *Geochim. Cosmochim. Acta*, 37, 1709-1733.

GIGGENBACH, W. F., 1988. Geothermal solute equilibria. Derivation of Na-K-Mg-Ca geothermometers. *Geochim. Cosmochim. Acta*, 52, 2749-2765.

KIM, G. Y., Y. K. KOH, C. S. KIM, D. S. BAE and M. E. PARK, 2000. Geochemical studies of geothermal waters in Yusung geothermal area. *Jour. Korean Soc. Groundwater Env.*, 7, 32-46 (in Korean).

LEE, J. H., 1999. *Geology of Korea*, Geological Society of Korea, Sigma Press, Seoul, 802p (in Korean).

REED, M. H., 1982. Calculation of multicomponent chemical equilibria and reaction processes in systems involv-

ing minerals, gases and an aqueous phase. *Geochim. Cosmochim. Acta*, 46, 512-528.

YUN, S. T., Y. K. KOH, H. S. CHOI, S. J. YOUM and C. S. SO, 1998. Geochemistry of geothermal waters in Korea: Environmental isotope and hydrochemical characteristics. *Econ. Environ. Geol.*, 31, 201-213.

Yongkwon Koh\*, Chunsoo Kim, Daeseok Bae and Kyeongwon Han

Korea Atomic Energy Research Institute, P.O. Box 105, Yuseong, Daejeon 305-600, Korea

\*Corresponding author: To: [nykkoh@kaeri.re.kr](mailto:nykkoh@kaeri.re.kr)